Chapter 4: Results and Discussion

4.1 ADSORPTION

4.1 1 Kinetics of Adsorption

The aim of the present study was to examine the batch adsorption characteristics of Ni (II) on wood ash. The study was conducted to investigate the effect of various factors like contact time, concentration, temperature and pH on the adsorption isotherm.

4.1.2 Effect of Ni (II) on wood-ash contact time and concentration

Adsorption is a slow process and adequate contact time is essential to allow the system to approach equilibrium. Each adsorbent particle has a certain capacity to adsorb, so that a higher dosages with less volume to treat per unit weight may reach equilibrium somewhat faster than the low dosages to yield valid points. In this study, the adsorption capacity of wood ash and contact time were studied. It was found that the removal of nickel from aqueous solution by adsorption increased with time(Fig.4.1). From this diagram it is observed that significant adsorption occurs in 60 minutes and that equilibrium is attained in approximately 120 minutes. From this study, the following observation were made:

1) The amount of Ni (II) adsorbed increases with time and reaches a peak. It remains constant at that level.
2) An adsorption time of 120 minutes has been found to be adequate for equilibrium to be attained in batch experiments.

It is further observed that the amount of Ni (II) adsorbed increases from 64.5% to 100% by decreasing the concentration of Ni (II) in the adsorbate solution from 2.07 m.mol to 0.17 m.mol. at pH 5 and 30^0C. The complete removal of Ni (II) was achieved at the low concentration of 0.17 m.mol.

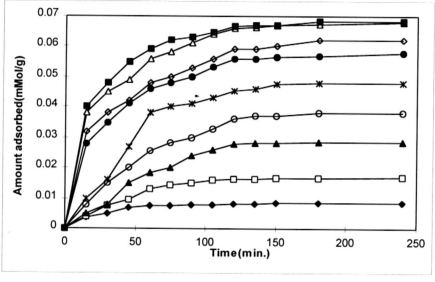

Fig. 4.1: Effect of time and concentration on Ni (II) removal by wood ash. The concentrations of Ni (II) were (■) 2.07, (Δ) 1.98, (◊) 1.72, (●) 1.55, (×) 1.21, (O) 0.86, (▲) 0.603, (□) 0.345, (◆)0.17 mmol respectively. Conditions: 30^0C and pH 5.

The adsorption characteristics of Ni (II) at various concentrations have been indicated in Fig. 4.1. The adsorption rate has been plotted as the amount of Ni (II) adsorbed (m.mol) per gm of the adsorbed against time.

The curves in Fig. 4.1 increase monotonically to saturation at various concentrations of Ni (II). This indicates the possibility of a monolayer adsorption of nickel on the outer interface of wood ash (Singh *et al.* 1984). The monolayer capacity of an

adsorbent is the quantity of adsorbate that can be adsorbed by one gram of the adsorbent in a "full-up" of monolayer .

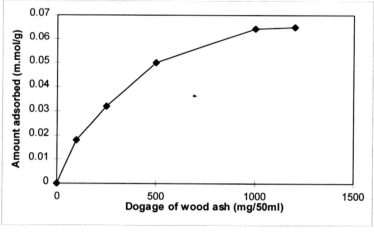

Fig. 4.2: Effect of dosage of wood ash on Ni (II) removal.

Fig. 4.2 shows that the removal of nickel increased from 25.0 to 64.5% under equilibrium when the dosage of the adsorbent was increased from 0.1 to 1.0 g per 50ml at an initial nickel concentration of 2.07 m.mol at pH 5 and at 30^0C.

4.1.3 Adsorption kinetics

The kinetics of Ni (II) adsorption on wood ash was studied in the light of the following equation.

$$\log (q_e - q) = \log q_e - k\,(t) \qquad (4\text{-}1)$$

This is similar to the Lagergren equation.

$$\log (q_e - q) = \log q_e - (k_1/2.3)\,t \qquad (4\text{-}2)$$

Where

qe = Amount of Ni (II) adsorbed (m.mol/g) at equilibrium

q = Amount of Ni (II) adsorbed (m.mol/g) at any time 't'

k_1 = Rate constant for adsorption

k = Rate constant of adsorption (Eqn. 4-1)

t = Time

Yadava *et al.*(1987) used Eqn. 4-2 to express the kinetics of removal of Cd (II) from effluent by flyash. The rate constants for the adsorption of nickel were determined from the plots of log (q_e - q) versus time. The linear plots of log (q_e - q) vs. t as shown in Fig. 4.3 (a-i)(pp89-91) at different nickel concentrations indicate the first order reversible kinetics. The average value of the rate constants were calculated from the slopes of the plots and found to be 3.71×10^{-2} min^{-1} at 30^0C. This observation conforms to the linear nature of the log(qe - q) vs. t plot obtained by Panday *et al.* (1985).

Minute variations in adsorption rate have been observed at various concentrations of adsorbate. Solution temperature exerts a significant influence on the rate of adsorption and low temperature favours the adsorption rate. In addition to surface adsorption, pore diffusion is often considered as a rate limiting step. The overall adsorption of Ni (II) generally involves the following steps:

(1) The transport by bulk diffusion towards the adsorbent

(2) Chemical reactions taking place at the external surface of the adsorbent

(3) Transport of the Ni (II) species into the internal surfaces of the micropores and capillaries of the adsorbent

(4) Chemical reactions taking place at the internal surfaces

In the present system, pore diffusion seems to be the rate limiting step because of sufficient mixing of adsorbate and adsorbent provided during the experiment. This was confirmed from the plots of amount adsorbed vs. square root of time at various concentrations and temperature (Fig. 4.4 a-i)(pp92-94).

According to Weber and Morris (1963), the initial curved portion and the subsequent linear portion of the plot represent the boundary layer adsorption and pore diffusion respectively. The rate constants of intraparticle transport (K_{id}) for the different concentrations of solution at different temperatures were determined from the slopes of the linear plots [Fig. 4.4.1(a-i), 4.4.2 (a-i) & 4.4.3 (a-i) at 20^0C, 30^0C and 40^0C respectively].These values are listed in Tables 4.1 (a, b, c) . It is clear from Table 4.1 that the value of the pore diffusion rate constant (K_{id}) increases with increase in initial adsorbate concentration and decreases with rise in solution temperature. The log-log plot of initial adsorbate concentration and rate constant for intraparticle transport (K_{id}) shows a linear relationship as shown in Fig. 4.5. In Fig. 4.4.1, 4.4.2 & 4.4.3 the straight lines were extrapolated to the x axis, as proposed by McKay *et al.*(1981) in their experiment to find out the extent of boundary layer adsorption. The values of the intercepts on the x-axis are proportional to the extent of boundary layer adsorption. The above findings clearly indicate that the boundary layer thickness and rate constants of intraparticle transport (K_{id}) decrease with respect to solution temperature. The adsorption process is exothermic in nature for the present system. The activation energy was determined from the slope of the Arrhenius plot, $\ln(K_{id})$ vs. 1/T as shown in Fig. 4.6 and was found to be -11.54 kJ mol^{-1} using the methodology of Tewary *et al.*, 1972.

Table 4.1(a) : K′ , K1 , K2 , Kid value for different concentrations at 20^0C

Concentration mMol/L	K′ Per min.	K_1 Per min. x 10^2	K_2 Per min. x 10^3	K_{id} mMol/g.(min.)$^{1/2}$
2.07	0.0409	2.73	13.6	0.61
1.98	0.0408	2.82	12.56	0.59
1.72	0.0484	3.57	12.67	0.55
1.55	0.0435	3.33	10.24	0.51
1.21	0.0424	3.57	6.7	0.42
0.86	0.0226	2.05	2.1	0.32
0.603	0.0548	5.23	2.5	0.24
0.345	0.0495	4.84	1.1	0.14
0.17	-	-	-	0.09

Table 4.1 (b) : K′ , K1 , K2 , Kid value for different concentrations at 30^0C

Concentration mMol/L	K′ Per min.	K_1 Per min. x 102	K_2 Per min. x 103	K_{id} mMol/g.(min.)$^{1/2}$
2.07	0.035	2.27	12.25	0.59
1.98	0.0334	2.26	10.79	0.58
1.72	0.032	2.31	8.943	0.51
1.55	0.0311	2.33	7.83	0.51
1.21	0.0306	2.53	5.3	0.42
0.86	0.0357	3.1	4.2	0.33
0.603	0.0518	4.896	2.835	0.25
0.345	0.043	4.19	1.25	0.15
0.17	-	-	-	0.08

Table 4.1 (c) : K′ , K1 , K2 , Kid value for different concentrations at 40^0C

Concentration mMol/L	K′ Per min.	K_1 Per min. x 102	K_2 Per min. x 103	K_{id} mMol/g.(min.)$^{1/2}$
2.07	0.0316	1.92	12.4	0.55
1.98	0.0316	1.99	11.65	0.54
1.72	0.0341	2.35	10.543	0.49
1.55	0.0385	2.73	11.18	0.46
1.21	0.024	1.92	4.8	0.37
0.86	0.0576	4.96	8	0.29
0.603	0.035	3.28	2.21	0.23
0.345	0.035	3.37	1.32	0.1
0.17	-	-	-	0.07

4.1.4 Adsorption Dynamics and Empirical Kinetic Model

The kinetic data obtained from the batch studies were mathematically analysed using an empirical model, similar to the one proposed by Prakash *et al.*(1987) and Yadava *et al.*(1988). The following model was employed to find out the rate of removal of Ni (II) from aqueous solution by adsorption on wood-ash at different concentrations.

$$\log(t+1) = B(Ci - C)^{A} \quad (4\text{-}3)$$

In which,

C_i = initial concentration of Ni (II) in water m.mol/L,

C = Concentration of Ni (II) in water at time t, in m.mol/L;

t = time in minutes;

B and A = empirical constants dependant on C_i.

The values of B and A were determined from the slopes and intercepts of the linear plots log[log(t+1)] versus log (C_i - C) as shown in Fig 4.7 (a-g) (pp102-104) .These plots can be expressed in the form of simple equations as given below:

For C_i = 2.07 m.mol , $\log(t+1) = 1.424 \times (C_i - C)^{1.2452}$ (4-4)

= 1.98 m.mol, $\log(t+1) = 1.532 \times (C_i - C)^{1.1773}$ (4-5)

= 1.72 m.mol, $\log(t+1) = 1.7771 \times (C_i - C)^{0.9172}$ (4-6)

= 1.55 m.mol, $\log(t+1) = 1.8625 \times (C_i - C)^{0.7924}$ (4-7)

= 1.21 m.mol, $\log(t+1) = 1.9364 \times (C_i - C)^{0.2547}$ (4-8)

= 0.86 m.mol, $\log(t+1) = 2.045 \times (C_i - C)^{0.2184}$ (4-9)

= 0.603 m.mol, $\log(t+1) = 1.8910 \times (C_i - C)^{0.1018}$ (4-10)

The plots of $\log_{10}$ (T+1) vs. $(C_i - C)^A$ are given in Fig.4.8 (a-h) (pp105-107) and the values of $\log_{10}$ (T+1) for the respective concentrations are shown in Table 4.2.

Table 4.2: The values of log (T+1) at various concentrations

Concentration Ci	**log (T+1)**
2.07	$1.424 \times (C_i - C)^{1.2452}$
1.98	$1.532 \times (C_i - C)^{1.1773}$
1.72	$1.7771 \times (C_i - C)^{0.9172}$
1.55	$1.8625 \times (C_i - C)^{0.7924}$
1.21	$1.9364 \times (C_i - C)^{0.2547}$
0.86	$2.045 \times (C_i - C)^{0.2184}$
0.603	$1.8910 \times (C_i - C)^{0.1018}$

It is observed from the above equations (4-4 to 4-10) that the empirical constant B varies considerably with initial concentration of adsorbate, whereas A decreases with increase in initial concentration. The percentage removal of Ni (II) with time can be found from the following equation:

$$\frac{(C_i - C) \times 100}{C_i} = \frac{100}{C_i}\left[\frac{\log(t+1)}{B}\right]^{1/A} \qquad (4\text{-}11)$$

The rate of Ni (II) removal is obtained from the equation given below:

$$-\frac{dc}{dt} = \frac{d}{dt}\left[\frac{\log(t+1)}{B}\right]^{1/A} \qquad (4\text{-}12)$$

The empirical constants, A and B are the functions of initial concentration (C_i) of Ni (II) in solution. In order to find out this relationship, log B vs. log Ci (Fig. 4.9) and A vs. Ci (Fig. 4.10) were plotted.

The variation of B with respect to initial concentration of Ni (II) is expressed by the following equation:

$$B = 0.295\ C_i^{0.1961} \quad (4\text{-}13)$$

and the variation of A can be expressed as:

$$A = 0.181 + 0.261\ C_i \quad (4\text{-}14)$$

4.1.5 Adsorption Isotherm

The adsorption data can be interpreted using several mathematical relationships which describe the distribution of the solute between the liquid phase and the solid phase.The equilibrium data for the adsorption of Ni (II) on wood-ash at 30^0C were fitted to Langmuir and the Freundlich isotherms as shown here.

Langmuir Isotherm:

$$\frac{Ce}{q_e} = \frac{1}{Q_0 b} + \frac{Ce}{Q_0} \quad (4\text{-}15)$$

Where Q_0 and b are Langmuir constants, which indicate the adsorption capacity and energy of adsorption respectively. The plot of Ce/qe versus Ce yields a straight line (Fig. 4.11) (p 108) at 30^0 C which confirms the applicability of the Langmuir isotherm. The values of Q_0 and b were obtained from the slopes and intercepts of linear plots and were found to be 0.492mM/g and 1.426 L/mM respectively. The equilibrium data were also fitted to the Freundlich isotherm. The mathematical form of the Freundlich isotherm is as follows:

$$q = K\ Ce^{(1/n)} \quad (4\text{-}16)$$

where,

q = amount adsorbate adsorbed per unit weight of adsorbent (m.mol/g)

Ce = Equilibrium concentration of adsorbate in solution after adsorption (m.mol/L)

K, n = empirical constants

The constants in this equation were determined by plotting q vs. C and employing Eqn. 4-16 rewritten as:

$$\log q = \log K + 1/n \log Ce \qquad (4\text{-}17)$$

which can be seen in Fig. 4.12. The value of the constants K and n were found to be 0.699 and 3.70 respectively.

4.1.6 Adsorption at various temperatures

The quantity of adsorbate that can be taken up by an adsorbent is a function of the nature and concentration of adsorbate and the temperature. Adsorption studies were conducted at 20^0 C, 30^0 C and 40^0 C to determine the influence of temperature on the adsorption of Ni (II) on the wood ash. The kinetics of Ni (II) adsorption on wood-ash at temperatures 20^0C and 40^0C were also studied using Eqn. 4-2. The linear plots of log (qe-q) versus t as shown in Fig. 4.13 and 4.14 at different concentrations for both the temperatures also indicate first order reversible kinetics. The average value of rate constants for 20^0C and 40^0C were calculated and found to be -0.0407 and -0.0355 respectively. Adsorption data from studies on Ni (II) adsorption on wood ash were found to fit well to the Langmuir isotherm at different temperatures (Fig. 4.15 and 4.16).

The validity of the Langmuir isotherm was further tested by regression analysis of the equilibrium data at various temperatures. The results are given in Tables 4.3 and 4.4.

Table 4.3: Ce/q_e value at different temperatures

Ce/q_e	Temperature (^{0}C)
14.01 + Ce/ 0.042	20
20.33 + Ce/0.0492	30
19.00 + Ce/0.053	40

Table 4.4: The value of the Langmuir constants at different temperatures

Temperature (^{0} C)	Qo (m.mol/g)	b (m.mol)	Regression Values	
			Qo	b
20	0.0424	1.678	0.0425	1.659
30	0.0492	1.426	0.0492	1.425
40	0.053	1.244	0.0531	1.234

The results indicate that the nickel adsorption capacity of wood ash decreases with increase in temperature, indicating that the adsorption process is exothermic in nature. This result is similar to the results obtained by Viraraghavan *et al.*(1991) and Yadava *et al.* (1987). The decreasing trend of adsorption with temperature may be due to the weakening of the adsorptive forces between the active sites of wood ash and nickel. Since physical adsorption is an exothermic process, an increase in the water temperature results in a decrease in the adsorption capacity. This indicates that the physical adsorption is a rate - determining step.

The essential characteristics of a Langmuir isotherm can be expressed in terms of a dimensionless constant separation factor or equilibrium parameter which is defined by Weber and Chakravorti (1974) as follows:

$$R = 1/(1+Qo\ Ci) \quad (4\text{-}18)$$

where,

Qo = Langmuir constant, and

Ci = Initial solute concentration(m.mol/g)

This parameter indicates the shape of the isotherm as follows:

Table 4.5: Shape of isotherm on the basis of R value. [Viraraghavan *et al.* (1991)]

Value of R	Type of Isotherm
R > 1	Unfavourable
R = 1	Linear
0 <R < 1	Favourable
R = 0	Irreversible

Table 4.6: Equilibrium Parameter " R" for Nickel adsorption on wood ash

Condition	R value
20^0 C	0.991
30^0 C	0.908
40^0 C	0.904

Table 4.6 shows the R values for the adsorption isotherms of nickel on wood ash .For nickel adsorption on wood ash , the R values are found to be less than 1 and greater than 0. This indicates favourable adsorption of nickel on wood ash in the temperature range of 20^0 C - 40^0 C.

The net change in enthalpy of adsorption ΔH is related to the Langmuir constant b as follows (Pandey *et al.*, 1985):

$$b \propto b' e^{-\Delta H/RT}$$

or

$$\ln b = \ln b' - \Delta H/RT \quad (4\text{-}19)$$

where b′ is constant.

The value of ΔH for the adsorption of Ni (II) on wood ash was calculated from the slope of the plot ln b vs. 1/T (Fig. 4.17) and was found to be -10.35 Kcal mol^{-1}. The negative value of enthalpy suggests that the adsorption process is exothermic in nature for the present system.

4.1.7 Thermodynamics Parameter

The various thermodynamic parameters have been calculated using the following equations:

$$\Delta G^0 = -RT \ln Kc \qquad (4\text{-}20)$$

$$\Delta H^0 = \frac{T_2 . T_1}{T_2 - T_1} \ln \frac{Kc_2}{Kc_1} \qquad (4\text{-}21)$$

$$\Delta S^0 = \frac{\Delta H^0 - \Delta G^0}{T} \qquad (4\text{-}22)$$

Where,

ΔG^0 = Change of free energy

ΔH^0 = Change of enthalpy

ΔS = Change of entropy

Table 4.7: Thermodynamic parameters at different temperatures

Temperature (^{0} C)	Thermodynamic Parameters		
	$-\Delta G^0$ (Kcal mol^{-1})	$-\Delta H^0$ (Kcal mol^{-1})	$-\Delta S$ (cal mol^{-1})
20	1.341	3.823	8.47

30	1.256	3.799	8.393
40	1.1732		

The equilibrium constants, Kc, Kc_1 & Kc_2 (ratio of K_1 and K_2 at temperatures 20^0, 30^0, & 40^0 C) were obtained from Table 4.1 (a, b, c). The negative value of free energy change (ΔG^0) at various temperatures (Table 4.7) indicate the spontaneity of the adsorption reaction. The negative values of enthalpy change, ΔH^0 (Table 4.7) show the exothermic nature of the Ni (II) adsorption on wood ash. Yadava *et al.*(1988) and Panday *et al.*(1987) suggested in one of their experiments that the negative entropy change, ΔS^0 (Table. 4.7) indicates faster interaction with the active surface sites of adsorbent (forward reaction). These findings are in accordance with the experimental results obtained from this study.

4.1.8 Adsorption at various pH values

The effect of the pH on the adsorption of nickel on wood ash was studied by varying the pH of the sorption mixture in the range 2 to 8. The pH was adjusted by addition of 0.1 M HCL or NaOH. The pH of the solution is an important factor in determining the rate of surface reactions, with the initial pH of the solution having more influence than the final pH. The effect of pH on the adsorption of nickel on wood ash may be explained on the basis of an aqua-complex formation owing to the oxides present in the ash (Rao *et al.*,1992). A positive charge develops on the surface of the oxides of the ash in an acidic medium as follows :

$$MO + H\text{-}OH \rightarrow M\text{-}OH_2^+ + OH^-$$

The effect of pH on the adsorption of nickel on wood ash is shown in Fig. 4.18. It is found that the removal of nickel by asdorption increase with the increase of pH from 2 to 5 at 30^0C temperature .These results agree with the result obtained by Low *et al* (1995).

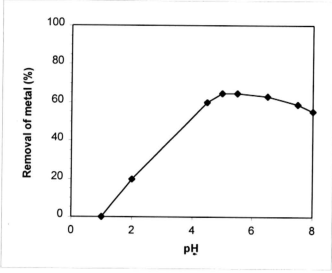

Fig. 4.18 Effect of pH on Ni removal by wood-ash from aqueous solution.

From Fig. 4.18, it is found that the extent of nickel removal at different pH shows a variation in the type of reactions involved with the varying pH values. The critical pH values was found to be between 4.5 to 5.5 . As pH decreased from 5 to 4.5 and further, the adsorption peak declined with the decrease in pH. This also indicates that the extent of nickel removal decreased. The variation of adsorption of nickel at various pH can be explained on the basis of metal chemistry in solution and the surface chemistry of the wood ash. The pH_{max} where maximum adsorption of the metal takes place seems to be related to the pK of the first hydrolysis product of the metal. The exact nature and distribution of hydroxo complexes depend on the concentration of the ligands i.e. solution pH and on the soluble metal concentration. In the pH range 4 to 5.5 , Ni^{+2} is the predominant species in solution. This in turn means that the variation in adsorption capacity in this pH range is largely due to the influence of pH on the surface adsorption characteristics of the wood ash.

It is evident that the surface charge of the ash becomes negative as a result of deprotonation of surface functional groups when the pH is raised within the range of 5 which can introduce electrical interaction into the positively-charged nickel ions

and negatively-charged wood ash. The ion-exchange reaction, in fact differs from adsorption. Since nearly every ion exchange process is accompanied by adsorption and desorption, adsorption sometimes is indistinguishable from ion exchange. Various theories have been put forward to describe and interpret metal ion interaction at solid solution interface. According to MacNaughton and James (1974), nickel is removed from aqueous solution by the following mechanisms:

(a) Ion exchange reaction

(b) Metal ion adsorption at hydrated oxides of the surface

(c) Metal hydroxyl species adsorption at the hydrated oxide surface.

In view of the above fact, it seems that the mechanisms (a) and (b) are more effective than (c) for the nickel-ash system because of the decrease in adsorption above pH 5.5. The decrease in adsorption of Ni (II) above pH 5.5 may be due to the formation of $Ni(OH)_2$. This is largely due to the fact that substantial precipitation of nickel as nickel hydroxide occurs at high pH values. The formation of hydroxide precipitate reduces the amount of free nickel ions which can bind to the wood ash.

4.1.9 Effect of coincidental anions and complexing agent

The effect of anions such as chloride, sulphate and complexing agents like EDTA on the adsorption of nickel to the biomass was studied. Sodium salts of these anions were employed in the experiments .As shown in Figs. 4.19 and 4.20 , the extent of interference in nickel adsorption varied with the type of anions present in the solution.

The two anions, namely sulphate and chloride, strongly inhibited nickel adsorption. Nickel adsorption decreased by approximately 30% in the presence of chloride at a concentration of 0.17mM. When sulphate was present at the same concentration,

nickel adsorption was reduced by 40%. This result was obtained at a maximum concentration of 0.17mM of $Ni_2(SO_4)_2$, which was equivalent to the initial concentration of nickel in the solution. Inhibition of nickel adsorption by the anions may be due to interaction of these anions with the heavy metal ions and/or with the surface of the wood-ash. Anions such as sulphate and chloride form weak complexes with positively-charged metal ions such as nickel. These complexes may not adsorb on the surface of biomass, resulting in a decrease in metal uptake by the biomass. The extent of complex formation between an anion and a metal ion depends on the pH of the reaction medium and the amounts of anion and metal present in the solution. This can be computed by solving the appropriate equilibrium relationship using the stability constants listed in Table 4.8.

Under the experimental conditions employed in this study, these calculations indicate that the fraction of nickel complexes are very small due to the small stability constants. Since the surface of the biomass (wood-ash) is amphoteric, negatively -charged anions can bind to positively-charged functional groups on the biomass surface. This process may subsequently hinder the uptake of nickel by the biomass. The extent of nickel reduction indicates that the binding of nickel is much more sensitive to the association of the anions and with the biomass surface. Since the electrostatic interactions dominate the binding mechanism of nickel, increasing anion concentration and hence ionic strength would lead to attenuation of these interactions, resulting in a reduction in nickel uptake.

Table 4.8: Stability constants of Nickel ligand complexes at zero ionic strength

Ligand	Stability Constant (log K,25^0 C) of Nickel	
Chloride	NiL	0.6
Sulphate	NiL	2.3
EDTA	NiL	20.4
	NiHL	24.0
	NiOHL	21.8

L = Ligand
(Morel and Hering ,1993)

Fig. 4.21 & 4.22 show the effect of the complexing agent EDTA on the adsorption of nickel. A rapid reduction in nickel uptake was obtained when the concentration of EDTA was varied from 0 to more than 0.17 m.mol/L. This uptake behaviour can be readily explained in terms of the formation of strong complexes among metal ions and complexing agents. The reactions in aqueous solution between EDTA and nickel ions occur very rapidly. It leads to the formation of complexes in simple 1:1 stoichiometry and are generally stable. This reaction is influenced by the pH of the system. The relative distribution of all species present in a system containing a complexing agent and a metal ion can be computed by solving a series of equilibrium equations using the appropriate stability constant listed in Table 4.8. In addition to pH, species distribution depend on the amount of the metal and complexing agent present in the system. For example, Fig. 4.23 shows a typical plot of species distribution computed for a system containing nickel at 0.17mM (10 mg/l) and pH 5 as a function of EDTA concentration. This calculation is based on the procedure given by Meites (1975). Table 4.8 shows a strong correlation between the amounts of free nickel remaining in solution and the levels of nickel adsorption in the presence of a specified amount of EDTA. This observation indicates that the

reduction of nickel adsorption is due to the formation of the negatively charged $NiEDTA^{2-}$ complex. At pH 5, the biomass surface bears the same charge as the $NiEDTA^{2-}$ complex, resulting in decreased adsorption due to electrostatic repulsion.

4.1.10 Effects of Coincidental Cations

Chloride salts of potassium and sodium were chosen to study the effect of cations on nickel adsorption since they are commonly found in metal finishing effluents. Fig. 4.24 shows the effect of the cations on nickel adsorption. Generally, the presence of these cations reduced nickel binding to the biomass. Maximum suppression was about 20%. In this study, the maximum cation to nickel molar ratio employed was 1:1. The suppression effect of these cations is expected to be greater if higher cation to nickel ratios are used.

4.2 SEPARATION OF NICKEL (II) SULFATE USING MEMBRANES

4.2.1 $NiSO_4$ Pressure and Permeate Flow Rate

The experiments were planned on the basis of available information of the concentration of heavy metals in electroplating wastewater in Malaysia. The concentration of Ni (II) in waste water varies from 10 to 50 mg/L (DOE, 1995). In the present work, three different concentrationS namely 10 mg/L, 30 mg/L and 50 mg/L, were used to study the permeate rate as against the pressure in a pilot plant. The objective of this work was to study the economic viability of using a membrane filter to recover heavy metals in concentrated form and water suitable for reusing in the process.

The membrane unit can withstand a maximum trans-membrane pressure (TMP) of 600 kPa without noise and vibration. The TMP was kept within the range of 100-600 kPa. The characteristic curve for the concentrations of 10mg/L,30mg/L and 50mg/L seen as Figs. 4.25 (a), (b) and (c) respectively show a general trend of increasing permeate flowrate with pressure. The trend was similar for the three concentrations tested. This is perhaps due to the fact that at such low concentrations of Ni, concentration polarization does not play a significant role. For example, when the Ni concentration was 10 mg / L (Figure 4.25 (a), the maximum pressure drop was observed as 490.0 kPa for a permeate flow rate of 7.57×10^{-5} m^3/ s and the minimum pressure drop 100.0 kPa for a permeate flow rate of 4.42×10^{-5} m^3/s. The increase in permeate flowrate with the pressure increases gradually up to a permeate flow rate of 7.57×10^{-5} m^3/s, beyond which the curve assumes a steady value, for the range of parameters, used in this experiment. This might be due to the high flux characteristic of the membrane which results in rapid convection of retained solutes

to the membrane surface, leading to well known phenomenon of concentration polarization (Porter, 1972).

For higher Ni concentrations, 30 mg/L and 50 mg/L, the characteristic curve for pressure versus permeate flow rate do not change significantly as shown in Figures 4.25 (b) and (c). For both these cases, the permeate flow increase slowly with the increase of pressure in the range of 5.05 x 10^{-5} m^3/s to 6.94 x 10^{-5} m^3/s. For a Ni concentration of 10mg/L, the pressure drop attains a value close to 490.0 kPa at permeate flow rates of 7.57 x 10^{-5} m^3/s or higher, whereas, for Ni concentration of 30 mg/L and 50 mg/L the pressure drop attains a value of 550.0 kPa at the permeate flow rate of 7.5 x 10^{-5} m^3/L or higher. These values of TMP drop and permeate flow rate indicate the range of parameters such as pressure drop and permeate flow rate to be employed to decide upon the best operating condition.

4.2.2 Pressure Drop and Ni in Permeate

As the trans-membrane pressure drop increases, the concentration of Ni in the permeate decreases. This behaviour is to be expected as for a given pore size distribution on the membrane surface, a higher pressure drop would cause a greater permeation of water molecules compared to Ni ions. For a Ni concentration of 10 mg / L as shown in Fig. 4.26 (a), the minimum amount of Ni in the permeate was 0.048 mg / L at a pressure drop of 490.0kPa. When the pressure drop decreased, the concentration of Ni increased slowly until the TMP drop of 350.0 kPa. In the range of 350.0 kPa to 150.0 kPa, the concentration of Ni increased rapidly to a level of 0.69 mg / L at 100.0 kPa.

A similar trend was observed for the feed concentration of 30 mg/L as shown in Fig. 4.26 (b) The concentration of Ni (II) in the permeate increased with the decrease of pressure. At a TMP 550.0 kPa, the minimum concentration of Ni (II) in the permeate was found 0.0276 mg/L while the concentration of Ni (II) in the permeate was 0.7013 mg/L at 100.0 kPa. It was found that the concentration of Ni (II) in the permeate decreased rapidly in the range of pressure 250.0 kPa to 400.0 kPa. A further rise in the TMP reduced Ni (II) concentration slowly in the permeate. The minimum amount of 0.0276 mg/L Ni (II) was obtained at a TMP of 550.0 kPa.

Figure 4.26 (c) shows the permeate versus TMP curve for a Ni feed concentration of 50 mg/L. The maximum concentration of 0.7097 mg/L Ni was observed at pressure drop of 100.0 kPa and the concentration decreased gradually with increasing pressure drop. A minimum value of 0.078 mg/L Ni in the permeate was obtained at a TMP of 550.0 kPa.

Similar observations were made by Paul (1972),and Matsuara (1981) . In all the cases, the concentration of solute in the permeate decreased as the trans-membrane pressure was increased. This phenomenon can be explained by the fact that both the solute and solvent molecules compete with each other to pass through the pores. Ni ions in the solution being larger in radii than water molecules have a reduced chance to pass through a pore. When the trans-membrane pressure drop is increased, the flow of water (solvent) increases as compared to that of Ni. Moreover, the smaller pores which contribute little to water permeation at low pressure drops also transmit significant amounts of water under high trans-membrane pressure drops.

4.2.3 Trans-membrane Pressure and Ni in Concentrate

The relationship between TMP drop and Ni in concentrate for feed concentrations of 10 mg/L, 30 mg/L and 50 mg/L are given in Figures 4.27 (a), (b) and (c) respectively. For a Ni concentration of 10 mg/L in the feed, a minimum concentration of 12.7438 mg/L of Ni in the concentrate was observed at a pressure drop of 100.0 kPa. The increment in pressure drop increased the amount of Ni in the concentrate gradually until the pressure drop reached 400.0 kPa. Beyond this, the increase of Ni concentration accelerated as shown in Figure 4.27 (a). A maximum amount of 16.1814 mg/L of Ni in concentrate was achieved at a TMP drop of 490.0 kPa.

For feed concentrations of 30 mg/L and 50 mg/L of Ni a gradual increase in Ni content in the concentrate was apparent {Figs.4.27(b) and (c) }. In Figure 4.27 (b) for a feed concentration of 30 mg/L, the concentration of Ni in the concentrate started from a minimum of 38.4685 mg/L at a TMP drop of 100.0 kPa and slowly increased until the TMP drop reached 250.0 kPa. After this, the Ni concentration increased rapidly to 45.0743 mg/L at a pressure drop of 400.0 kPa. A maximum of 48.9838 mg/L of Ni was obtained at a TMP drop of 550.0 kPa.

The observation for the feed concentration of 50 mg/L, starts with a minimum of 64.1627 mg/L of Ni in concentrate at a pressure drop of 100.0 kPa. The concentration increased gradually with increasing pressure drop until it reached a value of 500.0 kPa and a maximum concentration of 81.6194 mg/L of Ni was obtained at 550.0 kPa.

The effect of pressure drop on Ni in the concentrate also indicates the influence of concentration polarization which causes the accumulation of Ni ions at the membrane surface. This accumulation increases with increasing pressure drop. These ions carry the same charge and the repulsive force generated among them causes Ni ions to move away from the membrane interface. This action would reduce the transmission of Ni through the membrane.

4.2.4 Permeate Flow Rate and Ni concentration

An increase in permeate flow rate showed a reduction in Ni content in the permeate for all three feed concentrations. Figure 4.27 (a) shows the relationship between permeate flow rate and Ni content in the permeate,for the feed concentration of 10 mg/L. A maximum concentration of 0.69 mg/L of Ni was observed at the permeate flow rate of 4.426×10^{-5} m^3/s. The concentration of Ni decreased slowly with increasing permeate flow rate until a value of 5.05×10^{-5} m^3/s. A rapid reduction in Ni concentration was observed until the permeate flow rate reached 5.9×10^{-5} m^3/s. Further increase in permeate flow rate to 7.57×10^{-5} m^3/s resulted in a concentration of 0.048 mg/L. A similar result was obtained for the feed concentration of 30 mg/L, as shown in Figure 4.27 (b). In this case, the maximum concentration of Ni was 0.7013 mg/L at a flow rate of 4.42×10^{-5} m^3/s. The concentration of Ni decreased slowly to 0.5569 mg/L at a permeate flow rate of 4.9×10^{-5} m^3/s, and beyond this flow rate a rapid reduction in Ni concentration was observed.The concentration fell to 0.0648 mg/L at flow rate of 6.51×10^{-5} m^3/s. The Ni concentration in permeate reduced slowly until a minimum value of 0.0276 mg/L was observed at 7.57×10^{-5} m^3/s. The feed concencentration of 50 mg/L also gave an inverse relationship between the permeate flow rate and Ni in the permeate as shown in figure 4.27 (c). The maximum amount of Ni in permeate was 0.7079 mg/L at a flow rate of 4.42

$x10^{-5}$ m^3/s this dropped to a level of 0.078 mg/L at a permeate flow rate of 7.57 x 10^{-5} m^3/s.

A general explanation can be given to the filtration characteristic observed in this experiment. When permeate flow rate was increased, it allowed more water to pass through the membrane. The Ni concentration was reduced because it had to compete with the solvent molecule (water in this case) which is much smaller than Ni ions. The size of the solute ions becomes a disadvantage for the permeation process. Further more, the effect of concentration polarization also adds to the reduction of Ni concentration in the permeate.

The observed pressure drop vs. permeate flow rate characteristics for the three different feed concentrations have a similar pattern. This is an expected behaviour as the permeate flow rate increases with applied pressure drop. Owing to the limitation in the maximum allowable permeate flow rate of 7.5 x 10^{-5} m^3/s, the pressure drop characteristics could not be observed at a higher permeate rate. According to the solution-diffusion models, the pressure differential induces a concentration gradient of liquid within the membrane, and transport proceeds by simple Fickean diffusion (Paul, 1972).